Investigation of the structural anisotropy in a self-assembling glycinate layer on Cu(100) by scanning tunneling microscopy and density functional theory calculations

Mikhail Kuzmin[*,‡] *, Kimmo Lahtonen*[*], *Leena Vuori*[*], *Rocío Sánchez-de-Armas*[§], *Mika Hirsimäki*[*,+], *and Mika Valden*[*]

[*] Surface Science Laboratory, Optoelectronics Research Centre, Tampere University of Technology, PO BOX 692, FI-33101 Tampere, Finland.

[‡] Ioffe Physical Technical Institute, Russian Academy of Sciences, 26 Polytekhnicheskaya, St Petersburg 194021, Russian Federation.

[§] Materials Theory Division, Department of Physics and Astronomy, Uppsala University, P.O Box 516, S75120, Uppsala, Sweden

[+] To whom correspondence should be addressed: mika.hirsimaki@tut.fi

ABSTRACT: Self-assembling organic molecule-metal interfaces exhibiting free-electron like (FEL) states offers an attractive bottom-up approach to fabricating materials for molecular electronics. Accomplishing this, however, requires detailed understanding of the fundamental driving mechanisms behind the self-assembly process. For instance, it is still unresolved as to why the adsorption of glycine ([$NH_2(CH_2)COOH$]) on isotropic Cu(100) single crystal surface leads, via deprotonation and self-assembly, to a glycinate ([$NH_2(CH_2)COO-$]) layer that exhibits anisotropic FEL behavior. Here, we report on bias-dependent scanning tunneling microscopy (STM) experiments and density functional theory (DFT) calculations for glycine adsorption on Cu(100) single crystal surface. We find that after physical vapor deposition (PVD) of glycine on Cu(100), glycinate self-assembles into an overlayer exhibiting c(2 × 4) and p(2 × 4) symmetries with non-identical adsorption sites. Our findings underscore the intricacy of electrical conductivity in nanomolecular organic

overlayers and the critical role the structural anisotropy at molecule-metal interface plays in the fabrication of materials for molecular electronics.

Keywords: Cu(100), Glycine, Adsorption, STM, DFT, Self-assembly

1. Introduction

The self-assembly of organic molecules on metal surfaces has attracted increasing interest [1] since a bottom-up approach to building nanostructures offers several benefits over the top-down approach. In the field of molecular electronics, a great deal of attention has been recently paid to free-electron-like (FEL) states discovered at self-assembling molecule-metal interfaces. The FEL states in molecularly conducting systems typically exhibit an electron effective mass that is sensitive to the composition and structure of the adlayer. The electron effective mass, in turn, correlates with carrier mobility. By understanding how the metal substrate influences the conformation, reactivity, and bonding of organic layer, the carrier mobility in such systems could be tailored for specific purposes simply by modifying the substrate structure and composition.

Whereas clean metal surfaces, in general, do not exhibit FEL behavior [2], well-ordered molecular layers on metal surfaces may display FEL properties, thus making them conducive to fabrication of molecular electronics. For instance, adsorption of perylene-3,4,9,10-tetracarboxylic-3,4,9,10-dianhydride (PTCDA) on Ag(111) surface leads to the formation of a confined *isotropic* 2D interface state via hybridization of the lowest unoccupied molecular state of PTCDA and the well-known Ag(111) surface state [2-6]. Even more interestingly, an *anisotropic* FEL state can be induced in molecular layers on electronically *isotropic* substrates. In particular, upon adsorption at room temperature glycine ([$NH_2(CH_2)COOH$]),

the simplest of amino acids, undergoes a deprotonation reaction on Cu(100) and forms a well-ordered p(2×4) phase of glycinate ([$NH_2(CH_2)COO^-$]) molecules [7-18].

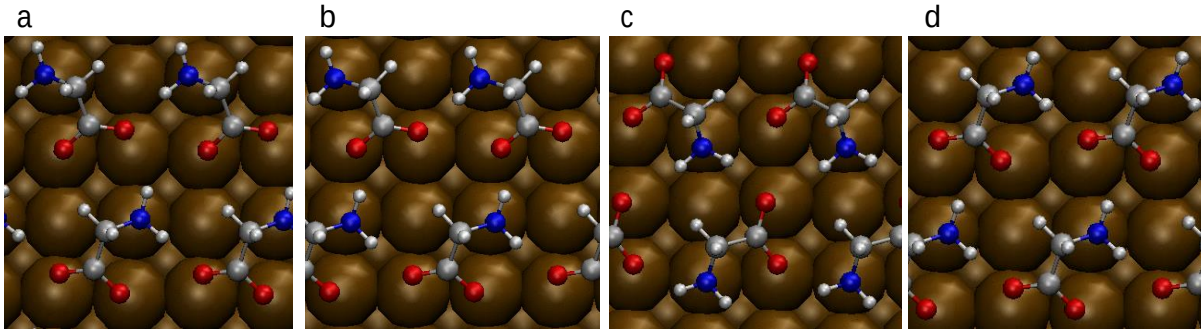

Figure 1. Earlier proposed molecular configuration for glycinate on Cu(100) [17]. Proposed alternatives are shown for p(2 × 4), Str-d (a), Str-h (b) and Str-3 (c) and c(2 × 4) (d) phases. For details see the text. Ochre, gray, blue, red and white spheres represent Cu, C, N, O and H respectively.

In their recent scanning tunneling microscopy and spectroscopy (STM/STS) experiments Kanazawa *et al*. reported strong *anisotropic* FEL dispersion relations for the p(2 × 4) phase, with the effective masses being different by one order of magnitude in [1 1 0] and [-1 1 0] directions [17]. The prospect of one being able to exert control over the degree of anisotropy in total or local electrical conductance by modifying the structure of molecular layers is an attractive one. To accomplish this goal does, however, require molecular level knowledge of the driving mechanisms behind the self-assembly process, details of molecular bonding and electronic structure.

The general consensus is that glycinate bonds with the Cu(100) surface in a tridentate configuration with the N atom of the amino group and both O atoms of the carboxylate group

bound to the metal substrate. The first structural model by Zhao *et al*. (called Str-d hereafter) was proposed for the p(2 × 4) phase on the basis of low-energy electron diffraction (LEED) and scanning tunneling microscopy (STM) [8]. The adsorption geometry is schematically illustrated in Fig. 1a. Although free glycinate does not exhibit chirality, two enantiomeric isomers are possible for glycinate adsorbed on Cu(100). Utilizing photoelectron diffraction (PhD) and reflection-absorption infrared spectroscopy, a slightly modified p(2 × 4) structure (Str-h, see Fig. 1b) was proposed by Kang *et al*. and Efstathiou and Woodruff [13,15]. In this structure the adsorption site of the molecules is identical to the adsorption site in the model of Fig. 1a. Density functional theory (DFT) based calculations performed by Mae and Morikawa argued for the structural model Str-d rather than the Str-h [14]. More recently, in an exhaustive DFT based computational study Zhi-Xin Hu *et al*. [18] concluded that the most likely structure of the p(2 × 4) phase is the arrangement shown in Fig. 1c (Str-3), where the O-O line in the glycine molecule is oriented roughly parallel to the longer edge of the p(2 × 4) unit cell. In this model, all molecules occupy identical surface sites and display the same conformation. However, some earlier experimental results hint of a more complicated scenario: there are two non-equivalent glycinate-related protrusions in STM images of the p(2 × 4) structure (e.g. see Fig. 2e in Ref. 16 and Fig. 4 in Ref. 18). It can be clearly seen in Figs. 1a, 1b, and 1c that heterochirality of glycinate in the earlier p(2 × 4) models cannot account for this STM observation, because of the mirror symmetry of the two adsorption configurations of the molecule. Therefore, the heterochirality cannot reconcile the earlier structural models with the experimental STM results. Moreover, simulated STM images for the earlier models give rise to the identical STM protrusions. This discrepancy is a serious obstacle to understanding the p(2 × 4) structure. Thus, in spite of considerable experimental and theoretical studies, the exact molecular arrangement of the p(2 × 4) glycinate phase so far remains under debate.

In this study we revisit the glycine's adsorption on Cu(100) by conducting *bias-dependent* STM measurements and DFT calculations. Our experimental findings show that the analysis of earlier STM results have missed evidence for two non-identical adsorption sites, which, in line with DFT calculations, suggest a novel asymmetrical p(2 × 4) model for glycine/Cu(100). In particular, two non-equivalent protrusions were observed in the p(2 x 4) structure, which were previously ascribed to STM tip effects or the heterochirality of the glycine molecules sitting at equivalent sites. However, our results indicated that the glycine molecules adsorbed on two non-identical sites of Cu(100) in the p(2 × 4) phase, which also leads to non-equivalent protrusions. Our results are consistent with the earlier STM, LEED, and PhD results in terms of molecular geometry. The non-identical adsorption sites thus offer a plausible explanation to the anisotropy of the surface and also suggest that glycine may have more than one p(2 × 4) phase on the surface.

2. Materials and methods

All experiments were performed *in situ* in an ultrahigh vacuum (UHV) system with a base pressure of $< 1\times10^{-10}$ mbar, equipped with a scanning tunneling microscope (UHV 300 Series VT-STM, RHK Technology Inc.) and an x-ray photoelectron spectrometer (ESCA3000 XPS, VG Microtech Inc.). The UHV system is described in more detail elsewhere [19]. A Cu(100) sample of 6*n* purity, cut to ±0.5° tolerance, was used. The Cu(100) surface was cleaned by repeated cycles of 10 min Ar^+ ion bombardment (2.0 kV, 15 μA) and 10 min electron beam annealing at 700 K. The sample temperature was monitored using *n*-type thermocouple attached in contact with the sample. The surface cleanness was verified by X-ray photoelectron spectroscopy (XPS) and STM. The step alignment was random and no tendency to form <310> steps, which will be considered in Sec. III, was seen. Typical terrace width as measured by STM was between 50 and 500 Å. STM was calibrated by measuring the known registry of Cu atoms on clean Cu(100).

The glycine was deposited on a clean Cu(100) substrate at 320 K via physical vapor deposition (PVD) from a crucible evaporator facing the sample. No further sample annealing was conducted. The glycinate coverage was estimated by XPS from N 1s signal that, in turn, was calibrated to the 0.5 ML saturation coverage of annealed Cu(100)-c(2 × 2)-N phase (1 ML = 1.53×10^{15} cm^{-2}) [20]. XPS also confirmed the presence of molecular glycinate on the surface (supporting information). The STM images were acquired in constant current mode at 300 K and were highly reproducible. Typical recording time was in the range of 3–7 min per image (200–400 ms per image line, 512 × 512 pixels per image, both scan directions measured). Several W tips were utilized.

All calculations were done using the VASP (Vienna ab initio simulation package) code [21-24] using the generalized gradient approximation (GGA) with the Perdew- Burke-Ernzerhof functional [25,26] and projector-augmented wave (PAW) potentials [27,28]. The valence electrons were described using a plane-wave basis set with a cutoff of 400 eV and 8x4x1 Monkhorst-Pack k-points set was used [29]. The Cu(100) surface was represented by a slab made of 2x4 unit cells and 5 layers (with the atoms of the 3 last layers fixed), and 10 layers of vacuum were added in the z direction to avoid the interaction between the slabs. Two glycinate molecules were placed only on one side of the slab and a dipole correction was applied. The geometries were relaxed until the net force on every atom was less than 0.01 eV/Å. Van der Waals interactions were taken into account through the DFT-D2 method of Grimme [30]. STM simulations were carried out using the Tersoff-Hamann approximation [31]. Constant-current STM images were finally visualized in the p4vasp program using an isosurface density of 0.005 $e/Å^3$.

3. Results and discussion

A 3D filled state STM image (a sample bias voltage -1.1 V) depicted in Fig. 2 represents the main features observed on the Cu(100) surface after the adsorption of glycine (coverage: 0.60 ML).

Firstly, the straight <310> steps, which are not found on the clean surface (see Sec. II), appear upon the adsorption. Secondly, these steps are bunched, resulting in the {3 1 17} facets, in good agreement with Refs. 8 and 16. The origin of the <310> steps and {3 1 17} facets was discussed earlier (see e.g. Ref. 16).

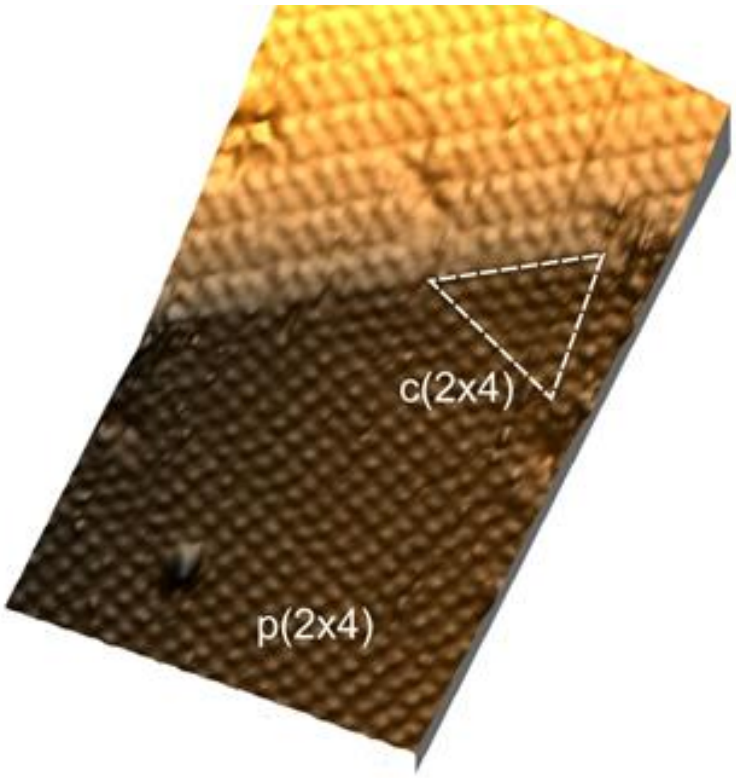

Figure 2. 3D filled-state STM image of the glycinate/Cu(100) surface at 0.60 ML coverage. One of domains of the c(2 × 4) structure is outlined. The sample bias voltage is -1.1 V and the tunneling current is 0.2 nA. The area is 18.8 nm × 11 nm.

Thirdly, two phases with different periodicities induced by adsorbed molecules are seen to coexist on the terrace in Fig. 2. One of these phases appears in the form of triangle shaped domain outlined by dashed line. The edge of this domain is always coupled to the <310>

step. The corrugation of this phase and its coupling to the <310> step are well consistent with the c(2 × 4) structure [8,16]. A model of this structure is shown in Fig. 1d. It is essential that in this model all the molecules have a similar chirality and occupy identical adsorption sites on the Cu(100) surface, so that the corresponding STM protrusions, as shown in Fig. 3a, have a similar appearance. The total energy of homochiral c(2 × 4) phase is very close to that of the heterochiral p(2 × 4) phase [14], and, thus, it is reasonable to consider the co-existence of the two adsorption phases [13,15].

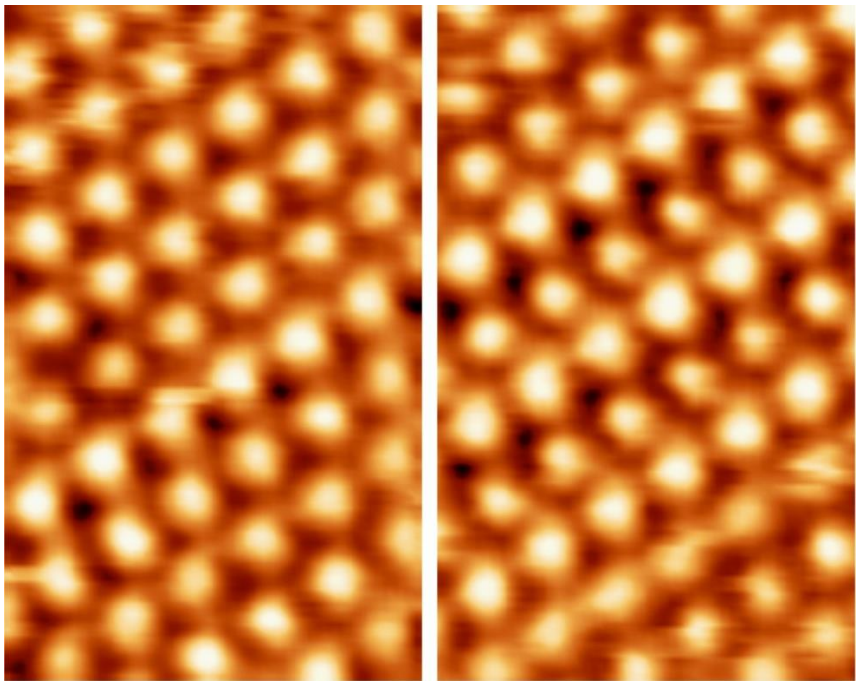

Figure 3. High-resolution STM images of (a) c(2 × 4) and (b) p(2 × 4) phases. The area of each image is 3.0 nm × 4.8 nm. The bias voltage is -2.0 V. The tunneling current is 0.40 nA.

A high-resolution STM image of the other observed phase is shown in Fig. 3b. It exhibits p(2 × 4) periodicity and consists of two alternating and dissimilar rows of protrusions. The average difference in height of protrusions between the adjacent rows is 0.05 Å, i.e., all the protrusions in the p(2 × 4) phase can be classified into two groups based on their brightness.

Obviously, the number ratio of such protrusions is 1:1. Moreover, the brighter and darker protrusions (they correspond to the Type-A and Type-B sites for the adsorbed molecules, respectively) have a different shape and the distance between the rows of brighter protrusions and the rows of darker protrusions is not constant, as is clearly seen in Fig. 3b. These properties of the p(2 × 4) phase are qualitatively different from the structural arrangement of the c(2 × 4) phase, where the inter-row separation is always constant and there is a single adsorption site (Type-A), as evidenced from the comparison of Figs. 3a and 3b.

These variations in brightness, shape, and inter-row separation clearly discriminate between the c(2 × 4) and p(2 × 4) phases, and we postulate that in the p(2 × 4) phase glycinate adsorbs at two non-equivalent sites and possibly in different configurations. On this basis we rule out the previously proposed p(2 × 4) models with a single adsorption site for the glycinate molecules (Fig. 1).

In order to gain insights into the molecular arrangement of the p(2 × 4) phase, we performed DFT calculations and compared the theoretical results with measured STM data. If considering geometric effects solely, the contrast of protrusions naturally indicates two different adsorption sites of the two glycine molecules in a supercell of the p(2 × 4) phase, different from that of previously proposed p(2 × 4) models where the two molecule are only in one site. A careful inspection of the registry of the STM protrusions in the p(2 × 4) and c(2 × 4) phases leads us to conclude that one adsorption site for the glycinate molecule in the p(2 × 4) is similar to that in c(2 × 4), and in previously proposed models in Fig. 1, whereas the other site is different.

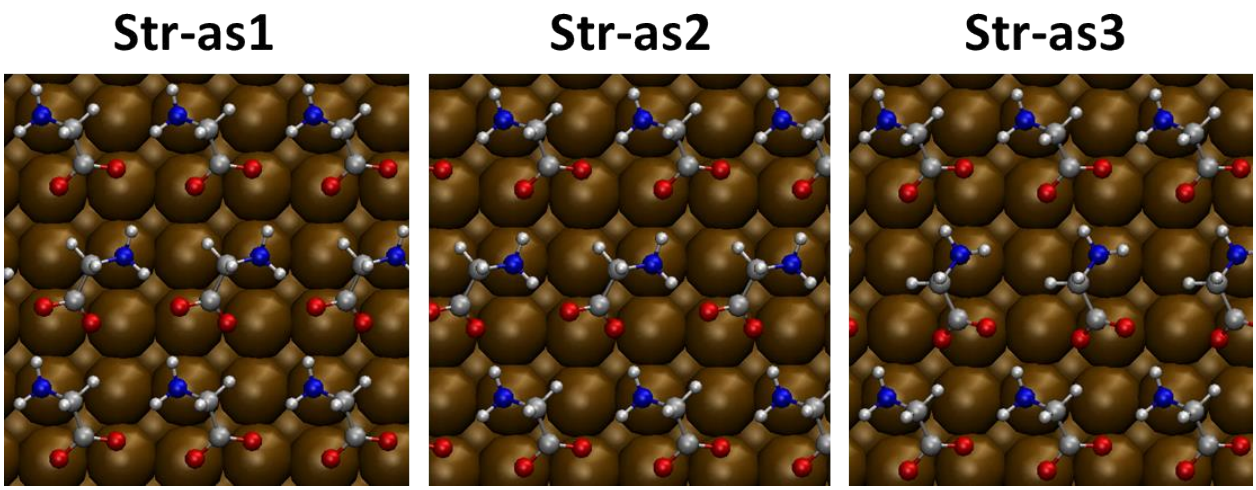

Figure 4. Three molecular asymmetric configurations considered of the p(2 × 4) surface with two inequivalent adsorption sites for the glycinate molecule (Str-as1, Str-as2 and Str-as3). Geometries were optimized at PBE-D2 level. Ochre, gray, blue, red and white spheres represent Cu, C, N, O and H respectively.

Based on the above analysis, four possible candidates for an asymmetric p(2 × 4) configuration, denoted as Str-as*N* (*N*=1,2,3,4), were considered. After structural relaxation, Str-as4 transforms into Str-as2, therefore, only three fully relaxed structures were obtained, as shown in Fig. 4. In each (2 × 4) supercell there are two inequivalent molecules labeled Type-A and Type-B. The detailed structural properties of all three configurations were summarized in Table 1. The main difference between Type A and Type B molecules is in the coordination of the two O atoms. In a Type-A molecule, one O atom resides at a Cu atop site and the other occupies an intermediate position in between the a-top site and a Cu bridge site, similar to that of previously reported Str-d and Str-h. For molecule Type-B, one O atom sits at the bridge site and the other is near the top site, as shown in Fig. 4. It leads to in a twisted molecule that the O over the top site is at least 1.0 Å higher than the bridge O. Therefore, the observed brightness modulation in STM images is, most likely, ascribed to the alternating

appearance of Type-A and Type-B molecules, as elucidated by simulated STM images (see below). Although there are two types of molecules in each asymmetric configuration, the similarity of N-Cu and C-Cu bond lengths might, in fact, be the reason for why Efstathiou and Woodruff did not observed two distinct types of molecules in their PhD experiments [15]. Among these three configurations, only the edge of Str-as3 is perfectly coupled with the <310> step.

Table 1: Calculated geometry for adsorbed glycinate. Z_N and Z_O are the vertical distances from N and O to the nearest Cu. d_{Cu-N} and d_{Cu-O} are Cu-N and Cu-O bond lengths, θ_N (θ_O) is the angle between Cu-N (Cu-O) bond and normal vector of the surface. Values for bridge-center coordinated O are given in parentheses. Geometry for the Type-A and Type-B configurations is visualized in Figure 5.

	PBE-D2						Exp.
	Str-as1		Str-as2		Str-as3		
	Type-A	Type-B	Type-A	Type-B	Type-A	Type-B	
Z_N(Å)	2.05	2.05	2.04	2.04	2.04	2.03	2.04 ±0.02
d_{Cu-N} (Å)	2.07	2.05	2.06	2.04	2.07	2.08	2.05 ±0.02
θ_N(°)	7.3	3.8	7.7	2.8	8.4	11.5	5 ±4
Z_O(Å)	2.02 (2.01)	2.98 (1.69)	2.05 (1.93)	3.09 (1.66)	2.08 (1.95)	1.57 (3.17)	2.02 ±0.02

d_{Cu-O} (Å)	2.04 (2.13)	3.06 (2.04)	2.09 (2.13)	3.21 (2.14)	2.10 (2.14)	2.05 (3.22)	2.05 ±0.02
θ_O(°)	8.8 (18.8)	12.7 (35.0)	10.4 (26.2)	16.0 (39.1)	9.5 (24.4)	36.17 (5.4)	9 ±2

Table 2: Calculated relative energies at PBE-D2 level of theory.

Configuration	Str-as1	Str-as2	Str-as3
Relative Energy (eV)	0. 0	0.05	0.25

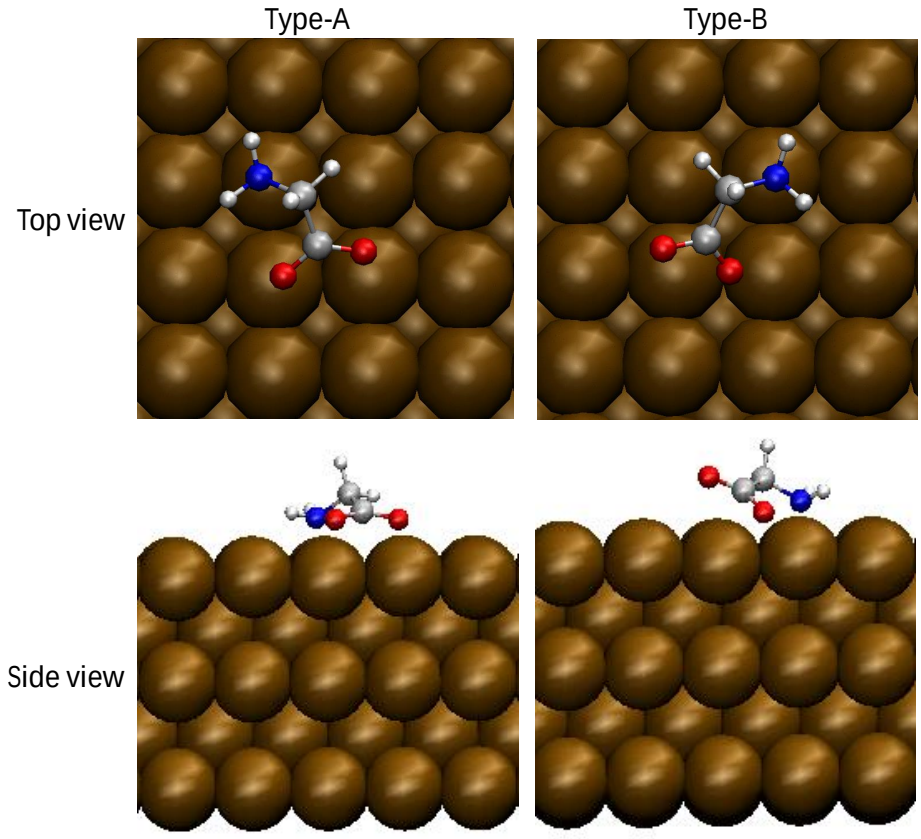

Figure 5. Visualization of the molecular geometry for Type-A and Type-B configurations as described in Table 1.

Total energies of the three asymmetric configurations are summarized in Table 2. Energetically, the proposed new structure (Str-as1) is just as viable as the previous Str-as2 structure wheras Str-as3 (0.25 eV) can be rejected. The good stability of Str-as1 is ascribed to that four electron affinitive atoms were involved in forming the hydrogen bonding square.

While the configuration Str-as1 is energetically viable among the three newly proposed configurations, however, it cannot be perfectly cleaved along the <310> direction. To obtain further evidence for the most likely structure, we performed high-resolution STM measurements at different bias voltages and compared the obtained bias-dependent STM images with those simulated by DFT calculations. The results are shown in Fig. 6.

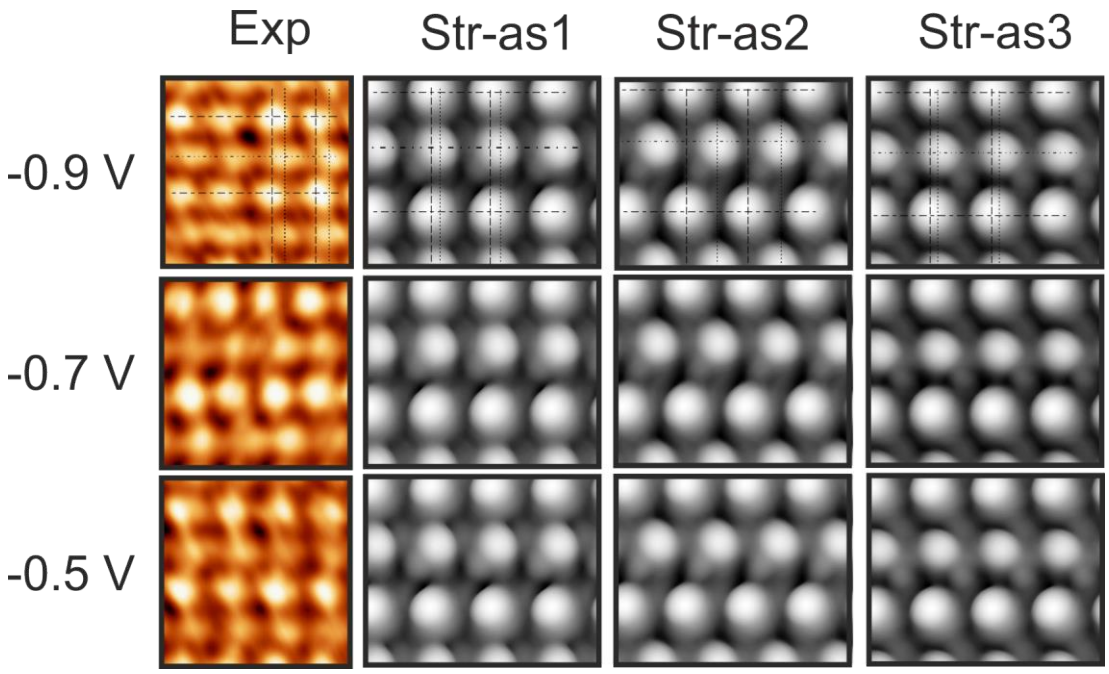

Figure 6. Comparison of experimental and simulated STM images. The experimental images are observed at bias voltages of -0.9, -0.7, and -0.5 V (the tunneling current is 0.50 nA). The simulated images are obtained for the Str-as1, Str-as2, and Str-as3 models in the energy ranges between the Fermi level and the respective bias voltages.

An isosurface of charge density at 5×10^{-5} e/Å^3 is plotted in the ranges between the Fermi level and the energy corresponding to the respective bias voltage. It is worth noting that the difference in brightness of STM protrusions is found to become more pronounced on the p(2 × 4) surface with decreasing absolute negative bias voltage. In other words, this difference is enhanced when probing the filled states with a bias voltage higher than -1.0 V. For this reason, STM images were measured at bias voltages of -0.9, -0.7 and -0.5 V. The appearance of protrusions was not affected by the scanning direction and was clearly reproduced with different STM tips. In Fig. 6 the images measured at each of the above bias voltages are compared with the respective images simulated for the three new models. Each pair of simulated and experimental images exhibits two different levels of protrusion brightness, i.e., two non-identical molecules in the p(2 × 4) supercell. In terms of observed different brightness of STM protrusions, the experiment-theory comparison rules out the earlier p(2 × 4) models and simulation if it does not arise from tip effects.

The calculated energies in Table 2 indicate that both Str-as1 and Str-as2 are viable candidates for the glycinate structure on Cu(100). Since the energies for Str-as1 and Str-as2 are near-identical, definitive conclusion cannot be drawn based on the calculated energy alone. However, by comparing the registries of protrusions in simulated and experimental STM images (shown by dashed lines in Fig. 6), we can reject the Str-as2. Thus, based on combined STM and DFT data, we can safely reject the Str-as2 and Str-as3 and assign the Str-as1 as the correct structural model for the p(2× 4) phase. It is worth noting that in this structure, molecular rows exhibit two different chiralities, *R* and *S*, which can be essential for understanding the properties of p(2x4).

Finally, we mention that the Str-as1 structure exhibits structural anisotropy, which allows us to suggest a natural explanation of the anisotropic FEL behavior of the p(2 × 4) surface. In other words, the *electronic* anisotropy that appears at the glycinate/copper interface on electronically isotropic Cu(100) substrate may correlate with the structural anisotropy in the p(2 × 4) arrangement. In contrast, it is difficult to see how the anisotropy could be reconciled by resorting to structural models featuring identical adsorption configurations as in Fig. 1. We argue that the earlier imperfection of experiment-theory comparison on electronic properties might be due to multiple p(2 × 4) configurations [17]. Further experimental and theoretical efforts aimed at the elucidation of the band structure are required in order to conclusively confirm the FEL behavior and to determine the role of the adlayer symmetry.

4. Conclusions

The major finding of this investigation is the novel p(2 × 4) model for the adsorption geometry of glycine, in the form of glycinate, on Cu(100) that revises the earlier models by re-introducing the concept of two non-identical adsorption sites and reconciles the discrepancy between experimental and simulated STM images. The brightness contrast of different rows in p(2 × 4) phase in STM measurements is considered for the first time. DFT calculations and simulated STM images indicte that the new model, called Str-as1, is the correct adlayer structure. This configuration, together with another less stable configuration Str-as3 that can be perfectly cleaved along the <310> directions, are able to reproduce the bias-dependent STM images reported here. In addition, their structural properties are also consistent with the earlier PhD results [15].

By showing evidence for two non-identical adsorption sites, we argue that glycinate self-assembles into the p(2 × 4) structure featuring qualitatively different molecular rows in the two perpendicular directions. To confirm the FEL behavior suggested by earlier STS

experiments and to clarify the role of adlayer structure in the anisotropy of electron effective mass, further investigations aimed at the elucidation of band structure of the glycinate-Cu(100) interface should be conducted by, for instance, means of angle-resolved photoelectron spectroscopy and *ab initio* electronic structure calculations. In particular, angle-resolved photoelectron spectroscopy would readily complement STS experiments, since in STS more than 90% of the measured tunneling current is contributed by the electronic states only near the Γ point.

ACKNOWLEDGMENT

The work was supported by Academy of Finland [grant number 250324].

REFERENCES

[1] J.V. Barth, G. Costantini, K. Kern, Engineering atomic and molecular nanostructures at surfaces, Nature 437 (2005) 671-679.

[2] R. Temirov, S. Soubatch, A. Luican, F.S. Tautz, Free-electron-like dispersion in an organic monolayer film on a metal substrate. Nature 444 (2006) 350-353.

[3] J. Zhao, M. Fent, J. Yang, H. Petek, The Superatom States of Fullerenes and Their Hybridization into the Nearly Free Electron Bands of Fullerites. ACS Nano 3 (2009) 853-864.

[4] W. Ji, Z.-Y. Lu, H. Gao, Electron core-hole interaction and its induced ionic structural relaxation in molecular systems under x-ray irradiation. Phys. Rev. Lett. 97 (2006) 246101.

[5] W. Ji, Z.-Y. Lu, H. Gao, Multichannel interaction mechanism in a molecule-metal interface. Phys. Rev. B 77 (2008) 113406.

[6] M.S. Dryer, M. Persson, The nature of the observed free-electron-like state in a PTCDA monolayer on Ag(111). New J. Phys. 12 (2010) 063014.

[7] X. Zhao, Z. Gai, R.G. Zhao, W.S. Yang, T. Sakurai, Adsorption of glycine on Cu(001) and related step faceting and bunching. Surf. Sci. 424 (1999) L347-L351.

[8] X. Zhao, H. Wang, R.G. Zhao, W.S. Yang, Self-assembly of amino acids on the Cu(001) surface. Mat. Sci. Eng. C 16 (2001) 41-50.

[9] G. Si-Ping, Z. Xue-Ying, G. Zheng, Z. Ru-Guang, Y. Wei-Sheng, Adsorption geometry of glycine on Cu(001) determined with low-energy electron diffraction and scanning tunnelling microscopy. Chin. Phys. 11 (2002) 839-845.

[10] Q. Chen, D.J. Frankel, N.V. Richardson, Chemisorption induced chirality: glycine on Cu{110}. Surf. Sci. 497 (2002) 37-46.

[11] X. Zhao, H. Yan, X. Tu, R.G. Zhao, W.S. Yang, Spillover-Induced Chemisorption of Amino Acid on Silver Surfaces. Langmuir 19 (2003) 5542-5545.

[12] R.B. Rankin, D.S. Sholl, Structures of Glycine, Enantiopure Alanine, and Racemic Alanine Adlayers on Cu(110) and Cu(100) Surfaces. J. Phys. Chem. B 109 (2005) 16764-16773.

[13] J.-H. Kang, R.L. Toomes, M. Polcik, M. Kittel, J.-T. Hoeft, V. Efstathiou, D.P. Woodruff, A.M. Bradshaw, Structural investigation of glycine on Cu(100) and comparison to glycine on Cu(110). J. Chem. Phys. 118 (2003) 6059-6071.

[14] K. Mae, Y. Morikawa, Stability of homochiral and heterochiral phases of glycinate

on Cu(0 0 1): a first principles theoretical study. Surf. Sci. 553 (2004) L63-L67.

[15] V. Efstathiou, D.P. Woodruff, Characterisation of the interaction of glycine with Cu(100) and Cu(111), Surf. Sci. 531 (2003) 304-318.

[16] K. Kanazawa, A. Taninaka, O. Takeuchi, H. Shigekawa, What Orchestrates the Self-Assembly of Glycine Molecules on Cu(100)?, Phys. Rev. Lett. 99 (2007) 216102.

[17] K. Kanazawa, Y. Sainoo, Y. Konishi, S. Yoshida, A. Taninaka, A. Okada, M. Berthe, N. Kobayashi, O. Takeuchi, H. Shigekawa, Anisotropic Free-Electron-Like Dispersions and Standing Waves Realized in Self-Assembled Monolayers of Glycine on Cu(100). J. Am. Chem. Soc. 129 (2007) 740-741.

[18] Z.-X. Hu, W. Ji, H. Guo, Molecular ordering of glycine on Cu(100): The p(2×4) superstructure. Phys. Rev. B 84 (2011) 085414.

[19] K. Lahtonen, M. Lampimäki, P. Jussila, M. Hirsimäki, M. Valden, Instrumentation and analytical methods of an x-ray photoelectron spectroscopy–scanning tunneling microscopy

surface analysis system for studying nanostructured materials. Rev. Sci. Instrum. 77 (2006) 083901.

[20] F.M. Leibsle, S.S. Dhesi, S.D. Barrett, A.W. Robinson, STM observations of Cu(100)−c(2×2)N surfaces: evidence for attractive interactions and an incommensurate c(2 × 2) structure. Surf. Sci. 317 (1994) 309-320.

[21] G. Kresse, J. Hafner, Ab Initio Molecular Dynamics for Liquid Metals. Phys. Rev. B 47 (1993) 558.

[22] G. Kresse, J. Hafner, Ab Initio Molecular-Dynamics Simulation of the Liquid-Metal-Amorphous Semiconductor Transition in Germanium. Phys. Rev. B 49 (1994) 14251.

[23] G. Kresse, J. Furthmuller, Efficiency of Ab-Initio Total Energy Calculations for Metals and Semiconductors Using a Plane-Wave Basis set. Comput. Mat. Sci. 6 (1996) 15.

[24] Kresse, G.; Furthmuller, J. Efficient Iterative Schemes for Ab Initio Total-Energy Calculations using a Plane-Wave Basis Set. *Phys. Rev. B* **1996**, *54*, 11169.

[25] J.P. Perdew, K. Burke, M. Ernzerhof, Generalized Gradient Approximation Made Simple. Phys. Rev. Lett. 77 (1996) 3865.

[26] J.P. Perdew, K. Burke, M. Ernzerhof, Erratum: Generalized Gradient Approximation Made Simple. Phys. Rev. Lett. 78 (1997) 1396.

[27] P.E. Blochl, Projector Augmented-Wave Method. Phys. Rev. B 50 (1994) 17953.

[28] G. Kresse, D. Joubert, From Ultrasoft Pseudopotentials to the Projector Augmented-Wave Method. Phys. Rev. B 59 (1999) 1758.

[29] H.J. Monkhorst, J.G. Pack, Special Points for Brillouin-zone Integrations. Phys. Rev. B 13 (1976) 5188.

[30] S. Grimme, Semiempirical gga-type density functional constructed with a long-range dispersion correction. J. Comp. Chem. 27 (2006) 1787.

[31] J. Tersoff, D.R. Hamann, Theory of the scanning tunneling microscope. Phys. Rev. B 31 (1985) 805.

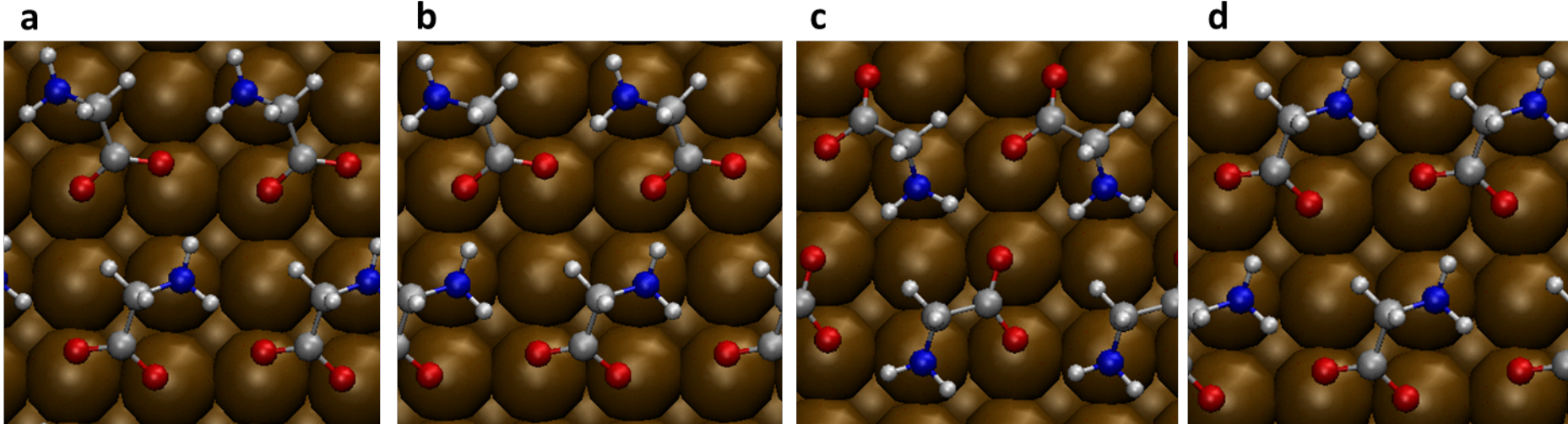
a
b
c
d

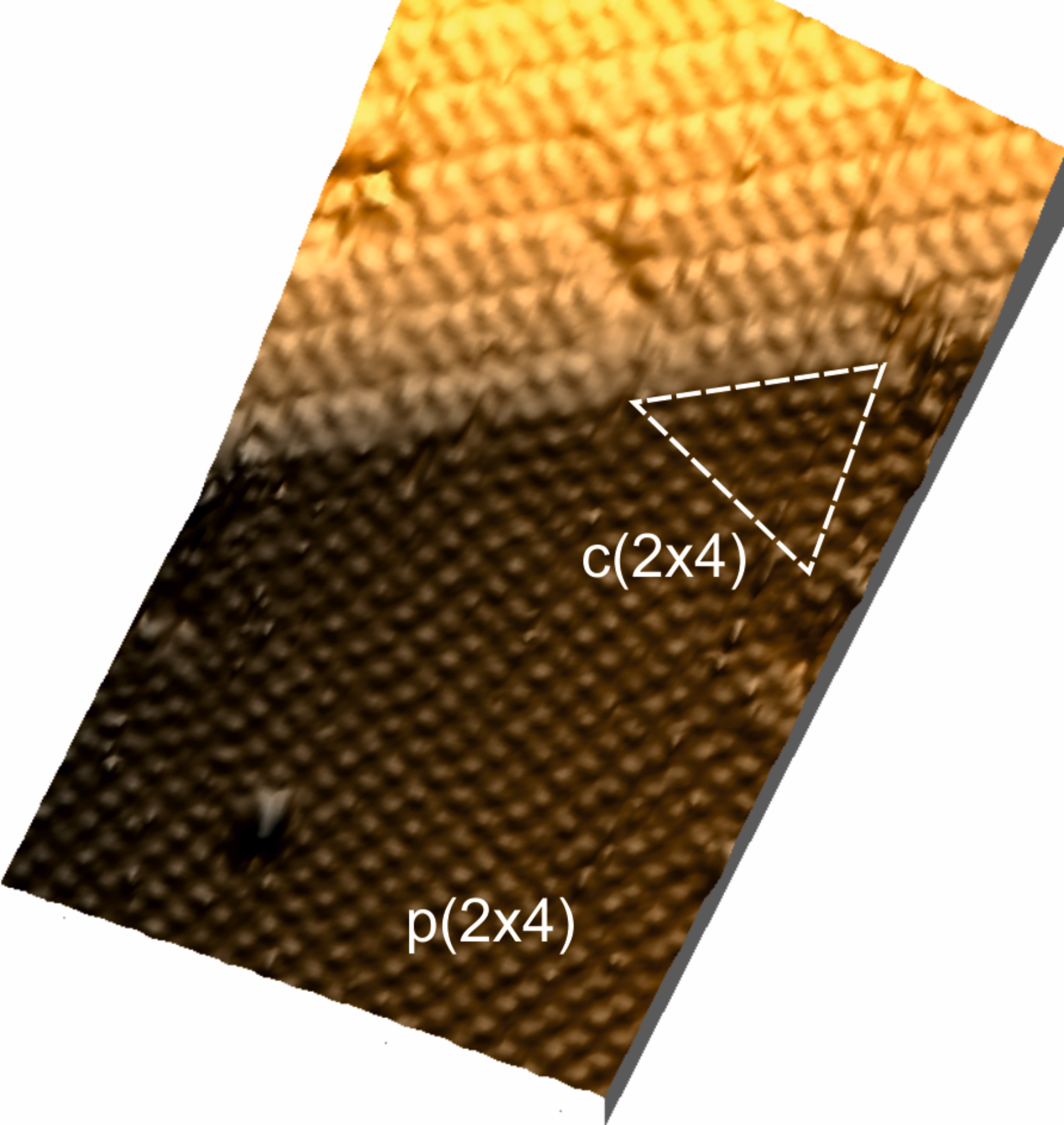
c(2x4)
p(2x4)

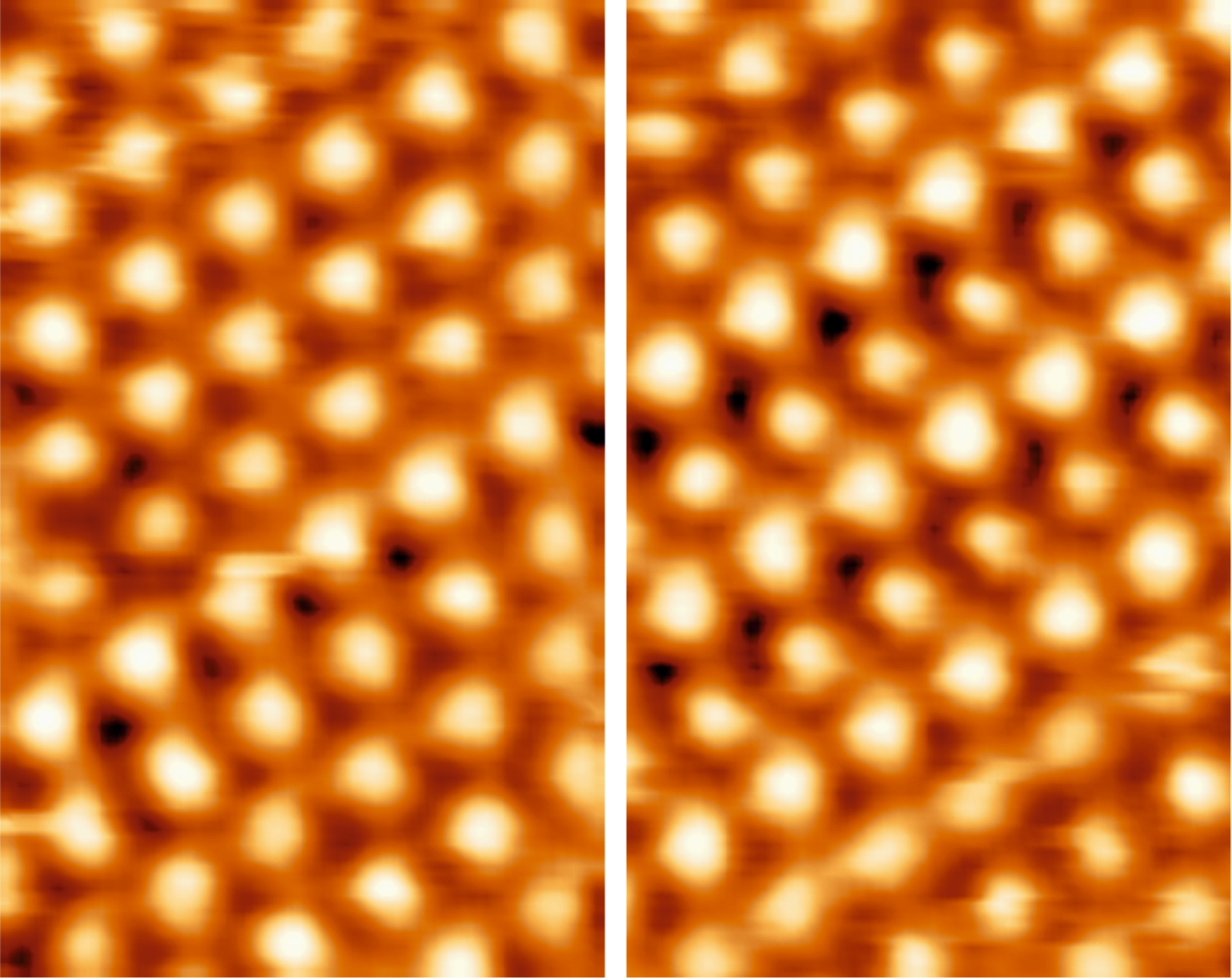

(a) (b)

Str-as1

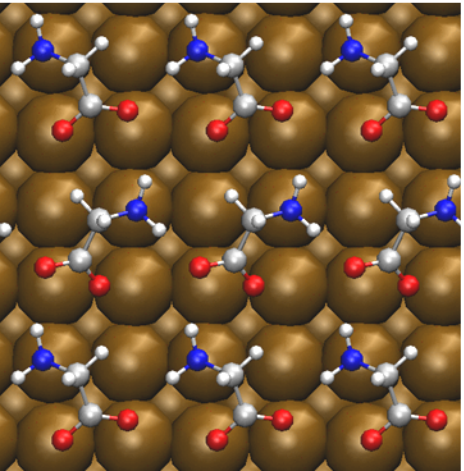

Str-as2

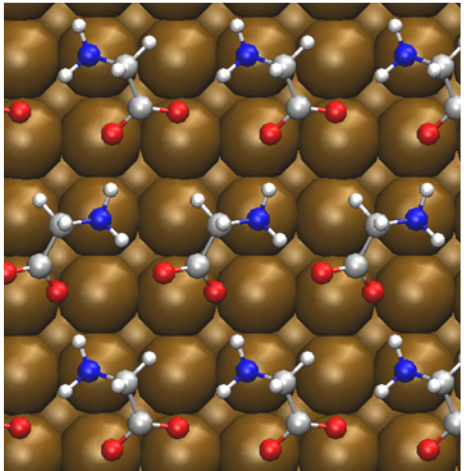

Str-as3

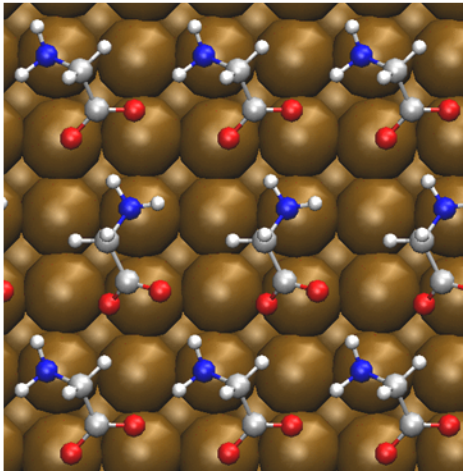

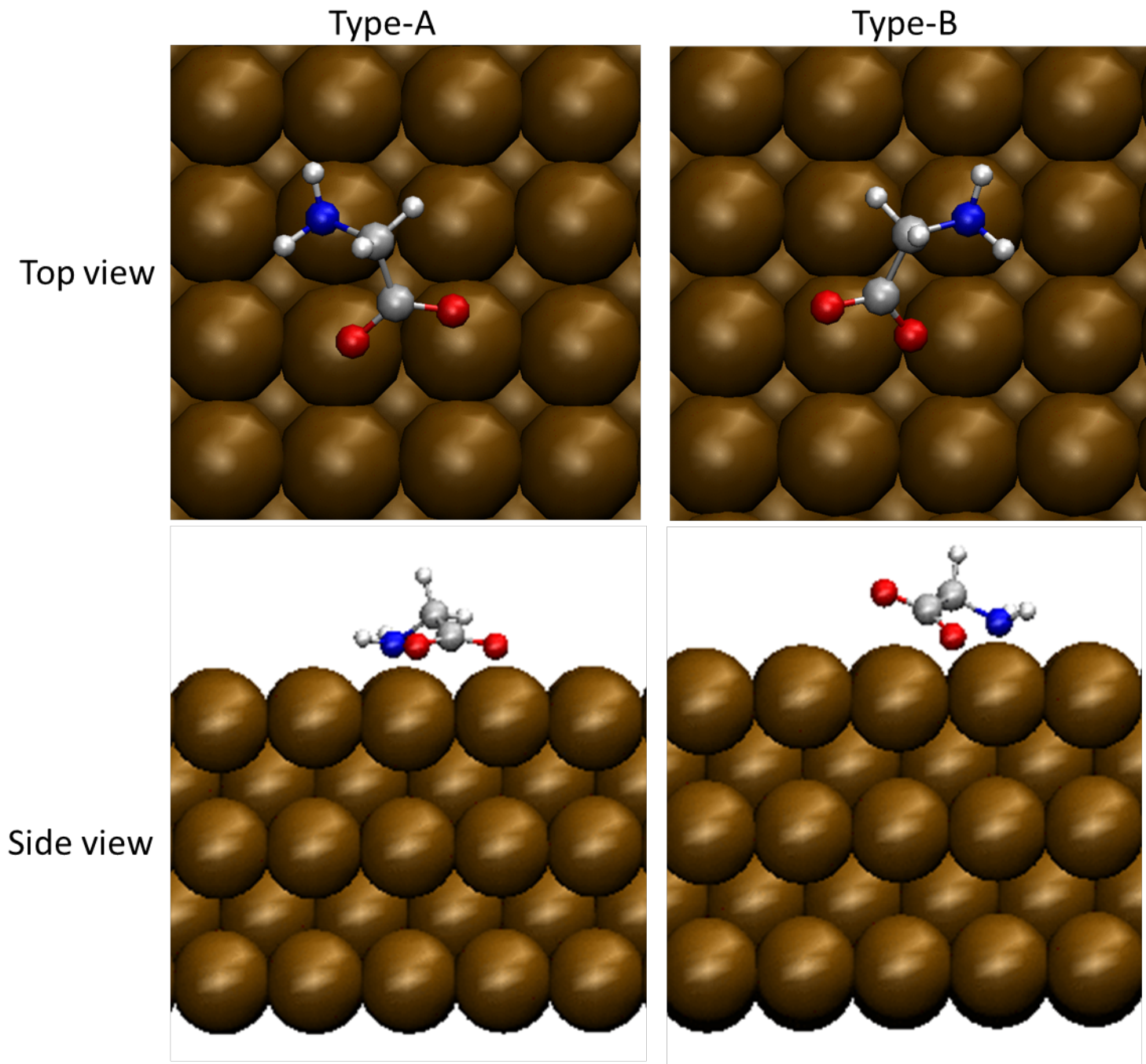
Type-A
Type-B
Top view
Side view

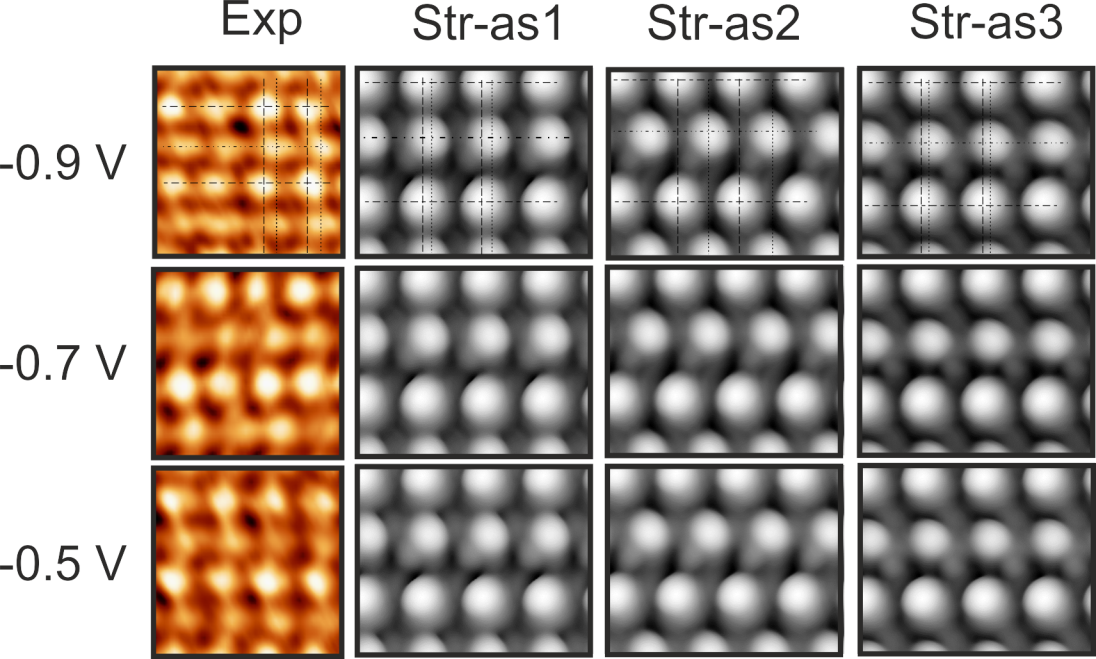
Exp
Str-as1
Str-as2
Str-as3
-0.9 V
-0.7 V
-0.5 V

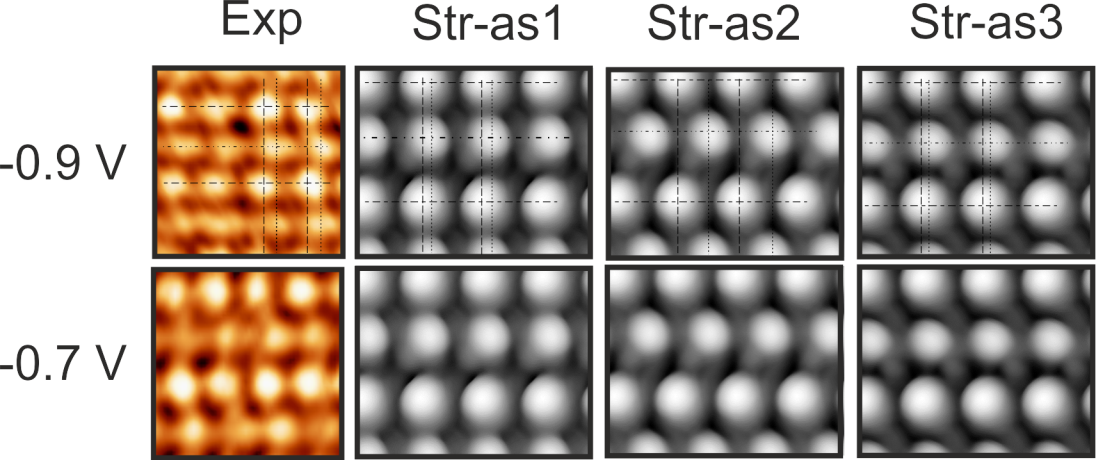
Exp
Str-as1
Str-as2
Str-as3
-0.9 V
-0.7 V

Supplementary Information for:

Investigation of the structural anisotropy in a self-assembling glycinate layer on Cu(100) by scanning tunneling microscopy and density functional theory calculations

Mikhail Kuzmin[*,‡], Kimmo Lahtonen[*], Leena Vuori[*], Rocío Sánchez-de-Armas[§], Mika Hirsimäki[*,+], and Mika Valden[*]

[*] Surface Science Laboratory, Optoelectronics Research Centre, Tampere University of Technology, PO BOX 692, FI-33101 Tampere, Finland.
[‡] Ioffe Physical Technical Institute, Russian Academy of Sciences, 26 Polytekhnicheskaya, St Petersburg 194021, Russian Federation.
[§] Materials Theory Division, Department of Physics and Astronomy, Uppsala University, P.O Box 516, S75120, Uppsala, Sweden

[+] To whom correspondence should be addressed: mika.hirsimaki@tut.fi.

Contents:

S-1: X-ray photoelectron spectroscopy (XPS)

XPS experiments were conducted on glycinate covered Cu(100) surfaces prior to STM experiments to identify and quantify chemical bonds in the glycinate layer. For subsequent STM experiments, the sample was transferred from XPS analysis chamber to STM chamber *in situ* to avoid atmospheric contamination.

Figure S-1 shows experimental C 1s signals after Shirley-background subtraction and the fitting of Gaussian peak shapes to quantify chemical bonds present on the surface. Table S-1 (page S4) summarizes the findings.

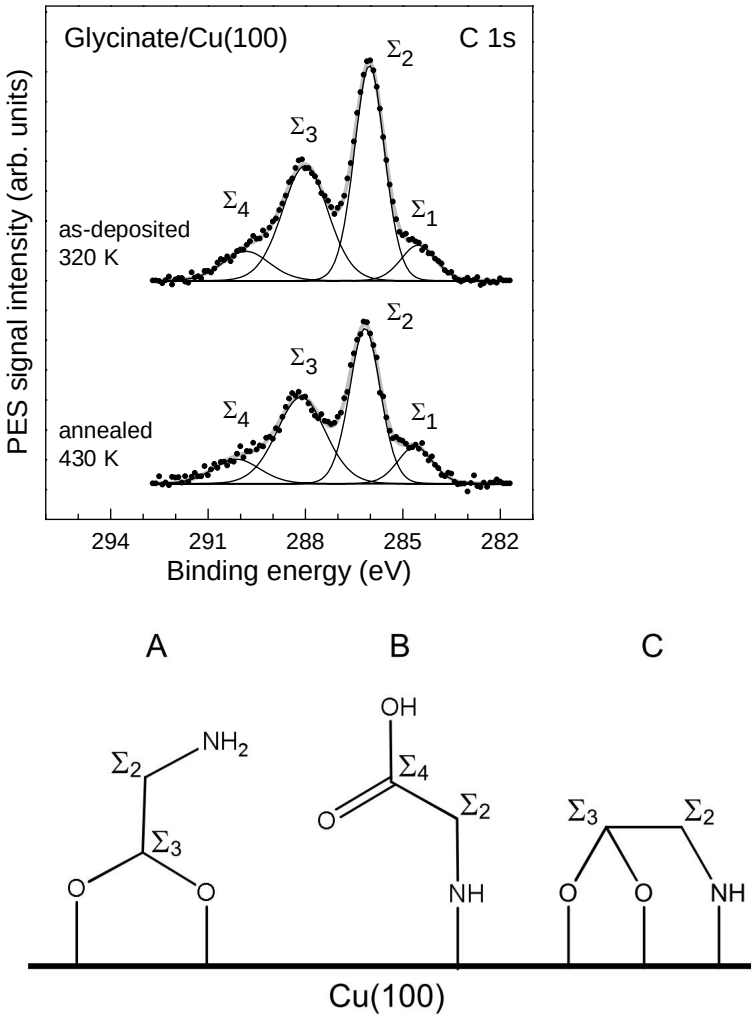

Fig. S-1 C 1s spectra and component fits obtained from glycinate/Cu(100) in as-deposited and annealed condition. Also shown is a schematic diagram of the three glycinate configurations as identified based on the C 1s bonds. The chemical bonds have been quantified in Table S-1.

The C 1s transitions shown in Fig. S-1 are resolved as:

Σ_1: hydrocarbons; C–C/H

Σ_2: carbon-nitrogen bond in glycine or glycinate; (O–)O–C–C–NH_2 (configuration A) or (HO–)O=C–C–

NH (configuration B) or (O–)O–C–C–NH (configuration C)

Σ_3: carbon-oxygen bond in deprotonated glycinate; (O–)O–C–C–NH_2 (configuration A) or (O–)O–C–C–NH (configuration C)

Σ_4: carbon-oxygen bond in protonated glycine; (HO–)O=C–C–NH_2 (configuration B)

XPS results show that the majority of the glycine molecules undergo a deprotonation reaction when adsorbed on Cu(100) as indicated by the higher intensity of Σ_3 in comparison to Σ_4.

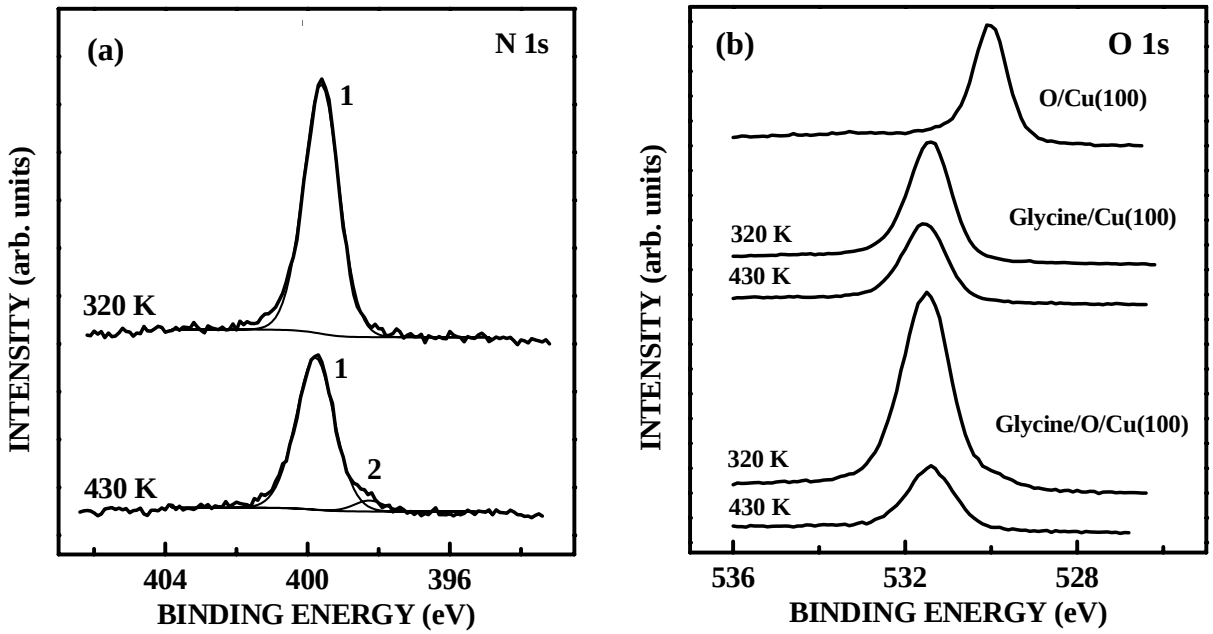

Fig. S-2 (a) N 1s and (b) O 1s signals as measured from glycinate/Cu(100). Also shown is O 1s signal from 0.5 ML O pre-covered Cu(100)-(2√2×√2)R45°-O reference.

Fig. S-2 shows N 1s and O 1s signals from glycinate/Cu(100) in as-deposited and annealed condition. The coverage of N and O is shown in Table S-1. N 1s signal originates predominantly from –NH_2 and CH_x-NH_x groups. O 1s signal from glycinate/Cu(100) exhibits a single state. It is distinct from dissociatively chemisorbed oxygen on clean Cu(100) as shown by the comparison with O 1s signal measured from O/Cu(100). Fig. S-2 also shows O 1s spectra measured after glycine adsorption on oxygen pre-covered Cu(100).

In summary, the XPS analysis was employed to elucidate the composition of the glycinate/Cu(100) prior to STM experiments and to confirm that the adlayer was identical in every experiment. Furthermore, the results indicated that the surface was predominantly covered by deprotonated glycinate (configurations A and C in Fig. S-1) as indicated by the strong Σ_3 spectral feature in the C 1s signal (Fig. S-1). However, the Σ_4 transition indicates that a fraction of the adsorbed glycinate has remained protonated (configuration B in Fig. S-1) even after annealing to 430 K.

Table S-1: Analysis of the chemical composition of the glycinate covered Cu(100).

Experiment	Component	Coverage (ML)	Concentration (at. %)	Binding energy (eV)	FWHM (eV)	Species
O/Cu(100)	O 1s	0.50	94.2	530.0	0.9	–O
Glycinate/Cu(100)	O 1s	0.63	48.7	531.4	1.2	–O
as-deposited	C 1s Σ_1	0.04	3.1	284.5	1.2	C–C/H
320 K	C 1s Σ_2	0.21	16.3	286.0	1.1	(*)
	C 1s Σ_3	0.17	13.2	288.0	1.7	(*)
	C 1s Σ_4	0.04	3.5	289.8	1.7	(*)
	N 1s Σ_1	0.19	15.1	399.6	1.2	$–NH_2$
	N 1s Σ_2	–	–	–	–	–
Glycinate/Cu(100)	O 1s	0.42	45.1	531.6	1.2	–O
annealed	C 1s Σ_1	0.04	4.5	284.6	1.2	C–C/H
430 K	C 1s Σ_2	0.16	16.8	286.2	1.1	(*)
	C 1s Σ_3	0.14	14.8	288.1	1.8	(*)
	C 1s Σ_4	0.04	4.0	290.1	1.7	(*)
	N 1s Σ_1	0.13	14.0	399.8	1.3	$–NH_2$
	N 1s Σ_2	0.01	0.8	398.3	1.0	$–CH_x–NH_x$

(*) See details in text under Fig. S-1.